Electrophoretic, Dynamic, and Static Light Scattering on Charged Polymer Emulsions

F.-M. C. LIN,* G. Ç. BERRY,† and R. L. FRYE,‡ *Department of Chemistry, Carnegie-Mellon University, Pittsburgh, Pennsylvania 15213* and L. C. SCALA, *Westinghouse Research and Development Center, Pittsburgh, Pennsylvania 15235*

Synopsis

Light scattering studies on dispersions formed by phase separation of a polymer-solvent-nonsolvent mixture show that the dispersions comprise charged droplets of the polymer-rich phase. The charge number is not large, and data on the electrophoretic-scattering and the dynamic scattering in the absence of an external electric field are both consistent with distribution of charge among the droplets. Data on the dependence of the static scattering on concentration and scattering angle show that the droplets are also disperse in radius. The data are discussed in terms of an interaction potential among the charged droplets relating the electrostatic interactions to the charge number and radius of the droplets, and the ionic strength of the solvent.

INTRODUCTION

It is well known that under certain conditions a homogeneous solution of a noncrystalline polymer can be caused to separate into two liquid phases, differing markedly in concentration and volume.[1] Under certain circumstances, the more concentrated phase may be formed as a reasonably stable suspension of small liquid droplets in the more voluminous dilute phase. In some cases, it is found that the suspended droplets so formed from an uncharged polymer will migrate in an electric field, providing a means for electrodeposition from solution.[2,3] Here, photon correlation light scattering experiments are reported for such systems, both in the presence and the absence of an external electric field.

Measurements of both the Rayleigh ratio $R(q, c)$ and the photon-count correlation function $g^{(2)}(\tau, q)$ are discussed below. Here q equals $(4\pi/\lambda)$ $\sin(\theta/2)$, with θ the scattering angle and λ the wavelength of light in the scattering medium, τ is the correlation time interval, and c is the polymer concentration (wt/vol). The function $g^{(2)}(\tau, q)$ is obtained from the photon-count rates $n(t)$ and $n(t + \tau)$ at times t and $t + \tau$, respectively, as[4-6]

$$g^{(2)}(\tau, q) = \langle n(t)n(\tau + t)\rangle_q/\langle n\rangle_q^2 \tag{1}$$

where the correlation is averaged over t and $\langle n\rangle$ is the average count rate. The Rayleigh ratio is proportional to the average count rate $\langle n\rangle_q$.

*Present address: Calgon Corp., Pittsburgh, PA.
†To whom correspondence should be addressed.
‡Present address: National Starch & Chemical Corp., Bridgewater, NJ.

Journal of Applied Polymer Science, Vol. 35, 1377–1397 (1988)
 CCC 0021-8995/88/051377-21$04.00

The suspended concentrated phase comprises droplets of polymer solution with concentration ρ (presumed to be the same in all droplets). With ν_α the number of polymer chains in the αth droplet, the product $M_\alpha = \nu_\alpha M_w^0$ represents the weight-average molecular weight of that droplet where M_w^0 is the weight-average molecular weight of the polymer. For the entire ensemble, the weight-average molecular weight M_w of the droplets is

$$M_w = c^{-1} \sum_\alpha c_\alpha M_\alpha = c^{-1} M_w^0 \sum_\alpha c_\alpha \nu_\alpha \tag{2}$$

where c and c_α are the total concentration and the concentration of droplets with molecular weight M_α, respectively. Insofar as the interchange of polymer chains among the droplets is slow, the light scattering may be treated as that from an ensemble of polymeric components, with M_w given by eq. (2).

With neglect of polydispersity among the droplet sizes, the Rayleigh ratio for the ensemble described above may be given by[4-6]

$$R(q, c) = KMcP(q, c)S(q, c) \tag{3}$$

$$S(q, c) = 1 - cB(c)W(q, c) \tag{4}$$

where K is an optical constant (see below), $P(q, c)$ accounts for intramolecular (intraparticle) interference, and $S(q, c)$ accounts for intermolecular (interparticle) interference. Both $P(q, c)$ and $W(q, c)$ are unity for zero q. If c is small, then $P^{-1}(q, c)$ and $S^{-1}(q, c)$ may each be expanded as a Taylor series in c giving the well-known expression[4-6,7]

$$\frac{Kc}{R(q, c)} = \frac{1}{M}\left[P^{-1}(q) + 2\Gamma_2 Q(q)c + \cdots\right] \tag{5}$$

where $P(q)$ and $2\Gamma_2$ are the limiting values of $P(q, c)$ and $B(c)$ for small c, respectively, and

$$Q(q) = \lim_{c=0}\left[\frac{W(q, c)}{P(q)} - \frac{1}{2\Gamma_2 P^2(q)}\frac{\partial P(q, c)}{\partial c}\right] \tag{6}$$

The effects of heterogeneity among the scattering moieties on $R(q, c)$ are considered in the Discussion.

For any type of solute, $P(q)$ may be expressed as[4-6,7]

$$P^{-1}(q) = 1 + q^2 R_{G,LS}/3 + \cdots \tag{7a}$$

$$R_{G,LS}^2 = M_w^{-1} \sum_\alpha w_\alpha M_\alpha R_G^2 \alpha \tag{7b}$$

where $R_{G\alpha}$ is the root-mean square radius of gyration of component α and $w_\alpha = c_\alpha/c$. For the system studied here, $P(q)$ for the droplet particles should be similar to $P(q)$ for a randomly branched chain. For example, if chains with a most-probable distribution of molecular weights are crosslinked at random

(short of gel formation), then[5,7,8]

$$P^{-1}(q) = 1 + q^2 R^2_{G,LS}/3 \tag{8}$$

exactly.

For linear flexible chain polymers, $Q(q)$ is nearly unity.[5-7,9] However, for monodisperse dense spheres, $Q(q)$ is not unity. Thus, for spheres,[5,6,10]

$$W(q,0) = \frac{\int_0^\infty r^2[g_0(r) - 1](\sin qr/qr)\,dr}{\int_0^\infty r^2[g_0(r) - 1]\,dr} \tag{9}$$

$$\Gamma_2 = (2\pi N_A/M)\int_0^\infty r^2[1 - g_0(r)]\,dr \tag{10}$$

where the particle pair distribution function $g_0(r)$ (at infinite dilution) is given by

$$g_0(r) = \exp[-V(r)/kT] \tag{11}$$

with $V(r)$ the interaction energy for spheres with centers separated by distance r. For monodisperse spheres, interacting through a hard-core potential [$V(r) = \infty$ for $r < 2R$ and zero otherwise],[10] $\Gamma_2 = 16\pi R^3 N_A/3M$ and

$$W(q,0) = \Phi(2qR) \tag{12a}$$

$$\Phi(X) = 3(\sin X - X\cos X)/X^3 \tag{12b}$$

By comparison, for such spheres, $P(q) = \Phi^2(qR)$. Since $P(q, c) = P(q)$ for dense spheres at any c, $Q(q) = \Phi(2qR)/\Phi^2(qR)$ in this case, and $Q(q) \approx P(q)$ for small q. Results obtained with $V(r)$ for charged spheres are discussed below.

In the following, use is made of an empirical correlation length $b(c)$ defined as

$$b^2(c) = -3\lim_{q=0} \frac{\partial \ln R(q,c)}{\partial q^2} \tag{13}$$

With the preceding expression, for small c,

$$b^2(c) = S(0,c)R_G^2 + [S(0,c) - 1]d^2(c) \tag{14a}$$

$$d^2(c) = -3\lim_{q=0} \frac{\partial Q(q)}{\partial q^2} \tag{14b}$$

$$S^{-1}(0,c) = 1 + 2\Gamma_2 c + \cdots \tag{14c}$$

In the infinite dilution limits, $b(0) = R_G$. For linear flexible chains $d(c) \approx 0$ and $b(c)$ decreases with increasing c (for $\Gamma_2 > 0$), or $b^2(c)S^{-1}(0,c)$ is expected

to be independent of c, and equal to $R^2_{G,LS}$, i.e., plots of $Kc/R(q, c)$ vs. q^2 for different c are all parallel.[5,7,9] For (monodisperse) dense spheres, $d^2(c) = 3R^2/5 = R^2_G$, so that $b(c)S^{-1}(0, c)$ is expected to be independent of c and equal to $R_{G,LS}$, i.e., the initial tangents of plots of $Kc/R(q, c)$ vs. q^2 are expected to decrease with increasing c.[15]

Both self-beating and reference beam photon correlation light scattering experiments[4-6] are used here to determine $g^{(2)}(\tau; q, c)$. In the self-beating experiments, $g^{(2)}(\tau; q, c)$ can usually be expressed as[5,6]

$$g^{(2)}(\tau; q, c) - 1 = [g^{(2)}(0; q, c) - 1]\left[\sum_\alpha r_\alpha \exp(-\gamma_\alpha \tau)\right]^2 \tag{15}$$

where $\Sigma r_\alpha = 1$, and the γ_α are conveniently expressed in terms of a scaling length a_α:

$$a_\alpha = \frac{q^2 kT}{6\pi \eta_s \gamma_\alpha} \tag{16}$$

with η_s the solvent viscosity and T the temperature [for convenience, notation for the dependence of r_α and γ_α (or a_α) on q and c is suppressed]. For a dilute suspension of monodisperse noninteracting spheres of radius R, only one term appears in eq. (15), with $a = R$.[4-6] With eq. (15), the limiting tangent for small τ is given by

$$\bar{\gamma}(q, c) = -\frac{1}{2} \lim_{\tau=0} \frac{\partial \ln[g^{(2)}(\tau; q, c) - 1]}{\partial \tau} \tag{17}$$

$$\bar{\gamma}(q, c) = \sum r_\alpha \gamma_\alpha \tag{18}$$

For a monodisperse solute, the scaling length $a(c)$ defined by eq. (16) can be expressed for $qR_G \ll 1$ as

$$a(c) = a_0 \frac{S(0, c)}{1 + G(c)[S(0, c) - 1]} \tag{19}$$

[for $S(0, c) \neq 1$], where a_0 is the limiting value of $a(c)$ for small c and $G(c)$ and $S(0, c)$ are both unity at infinite dilution. In many cases, $G(c)$, which includes the effects of hydrodynamic interactions, is not far from unity, so that the variation of $a(c)$ with c is expected to be small.[5,6]

With a reference beam experiment,[4-6,11]

$$g^{(2)}(\tau; q, c) - 1 = [g^{(2)}(0; q, c) - 1] \times \sum_\alpha r_\alpha \exp(-\gamma_\alpha \tau) \sum_\mu P_{\alpha\mu} \cos \Delta\omega_{\alpha\mu} \tau \tag{20}$$

where $\Sigma r_\alpha = 1$ and, for each α, $\Sigma P_{\alpha\mu} = 1$. The several parameters appearing in eq. (20) are discussed below. Here we remark only that $\Delta\omega_{\alpha\mu}$ is associated with

some uniform motion of the scattering centers. In this study this motion will be caused by application of an electric field, and $\Delta\omega_{\alpha\mu}$ will be proportional to the electrophoretic mobility. Equation (20) allows for a range of $\Delta\omega_{\alpha\mu}$ for the contribution to $g^{(2)}(\tau; q, c)$ attributed to a particular γ_α.

EXPERIMENTAL

Polymers used included polyamides with the structure

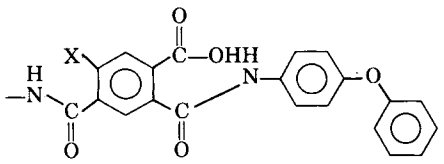

where —X is —COOH (I) or —H (II), polysulfones with the structure

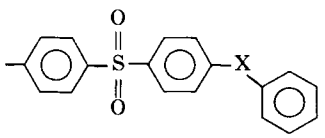

where —X— is —O— (III) or $-C(CH_3)_2-$ (IV), and the poly(parabanic acid)

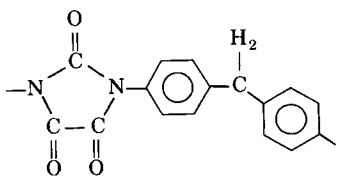

(V)

These were obtained from various sources: I, duPont de Nemours (Pyre-ML, RC5057); II, Amoco (AI-10HL); III, ICI America, Inc. (Victrex 300P); IV, Union Carbide, (Radel 5000); and V, Exxon (PPA-M, Batch E-59363).

Solutions were prepared by dissolution of the appropriate weight of polymer in the solvent or, in some cases, by dilution of a stock solution provided by the supplier. The solution was delivered into a stirred nonsolvent to create a suspension of the precipitated phase. The polymer solution was added to the nonsolvent at a rate of 2–3 mL/s, with rapid mixing. Typically, the polymer concentration c in the mixed solvent was 5–8 g/kg. In the suspended phase collected by centrifugation, the polymer concentration was about 200 g/kg (the supernatant contained no polymer). If prepared with the proper balance of agitation and rate of addition, the suspensions were essentially stable over a

period of days, see below. In applications involving electrodeposition of the suspended concentrated phase, it was found that the presence of an alkylamine often increased the deposition rate.[2,3] As a consequence, some of the preparations studied here contained such an amine. The compositions studied are given in Table I.

Measurements of $R(q, c)$ were carried out as a function of θ using cylindrically symmetric light scattering cells described elsewhere.[5,12,13] The depolarized light scattering was small, indicating that multiple scattering is not significant in the systems studied.

A schematic diagram of the light scattering cell used for measurements of the electrophoretic mobility is given in Figure 1. The cell is similar to one used in prior studies.[14] The rectangular section of the cell (c) was fabricated from rectangular Pyrex-glass tubing (Vitro Dynamics, Inc., Rockaway, NJ), with the rectangular section being 0.03 cm thick, 1 cm wide, and 1.4 cm long. The frits (F) are designed to prevent gas bubbles originating at the platinum electrodes from entering the cell. Since bubble formation was not a problem in the system studied (see below), the frits were removed in some experiments discussed here.

Except for modifications discussed below, the light scattering method, apparatus, data acquisition system, and correlator are described in detail elsewhere.[5,12,13] The vertically polarized 514.5 nm line of an argon-ion laser was used as the incident beam. In order to conduct reference beam experiments, a portion of the incident beam was reflected onto a mirror by a thin inclined plate (a microscope slide cover slip) placed in the incident beam. This beam was then expanded, and a portion of the image directed down the optic axis of the detector by the use of another thin inclined plate, so that the reflected image was superposed on the image of the scattering cell in the plane of the photomultiplier. In reference beam experiments the granite table top on which the photometer is mounted was supported pneumatically to minimize vibrations. A pulse from the data acquisition system timed to coincide with the data acquistion period was used to trigger a circuit to impress voltage V on the electrodes in the electrophoretic light scattering cell, see below.

The photon-count correlation function $g^{(2)}(\tau, q)$ was determined as[5,12,13]

$$g^{(2)}(\tau, q) = G^{(2)}(\tau, q)/\langle n\rangle_q^2 \tag{21}$$

$$G^{(2)}(\tau, q) = \frac{1}{M}\sum_{j=1}^{M}\left(\frac{1}{T}\sum_{i=1}^{I} n_i n_{i+k}\right)_j \tag{22}$$

where $\tau = k\Delta\tau$, with k an integer and $\Delta\tau$ the sampling interval, $\langle n\rangle$ is the average count rate, $T = 2^{12}$, and M was adjusted so that the total number of counts $\langle n\rangle$ TM was about 10^6. In most experiments the maximum value k was 32. Values of $\Delta\tau$ were chosen in successive experiments to permit evaluation of any curvature in $\ln[g^{(2)}(\tau, q) - 1]$ vs. τ over the range for $g^{(2)}(\tau, q) - 1$ greater than about 0.001 in self-beating experiments, with a similar criterion in reference beam experiments.

Most of the reference beam experiments were carried out with an apparent scattering angle θ_{APP} of 30°. Owing to refraction, the actual scattering θ is

TABLE I
Emulsion Compositions

Emulsion	Polymer[a]	Solvent[b]	Nonsolvent[b]	Other[b]
1	I	NMP (32)	Acetone (68)	TEA
2	II	NMP (20)	Acetonitrile (80)	—
3	II	NMP (9.3)	Ethylacetate (90.7)	—
4	III	NMP (18)	Acetone (82)	—
5	IV	NMP (35)	Acetone (65)	TEA
6	V	DMF (25.7)	Acetone (74.3)	TEA

[a]See text for structures.
[b]DMF = dimethyl formamide; NMP = *N*-methyl pyrrolidone; TEA = triethylamine; (2–4%) ( ) = wt % of component in solvent/nonsolvent mixture.

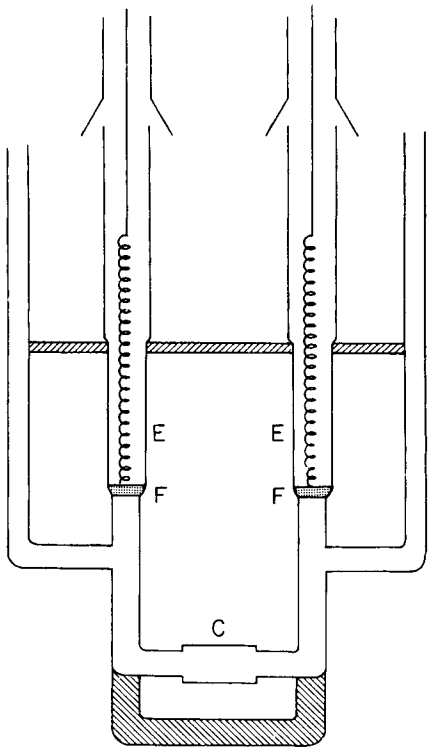

Fig. 1. Schematic diagram of cell used for electrophoretic light scattering: C = a thin, rectangular tube section connected to frits F by small-bore tubing with electrodes E above the frits (from Ref. 5).

smaller than θ_{APP}, with

$$\theta = \arcsin\left(n^{-1}\sin\theta_{APP}\right) \tag{23}$$

where n is the refractive index of the scattering medium; an Abbe refractometer was used to determine the latter. Most of the reference beam experiments were made with $\theta \approx 20°$, or $q^{-1} \approx 170$ nm.

A constant voltage power supply (Kepco, Model ABC 425M) was used to impress a voltage V across the electodes, from which E was determined as $E = V/d$, with d the length of the rectangular cell (c). The voltage was applied as a pulse using a circuit triggered by a pulse from the data acquisition system used with the light scattering apparatus. Provision was made to alternate the polarity of V in successive experiments to avoid net translation of the particles. The specific conductance κ_{SP} of the dry solvents used in this study was low (e.g., about 5×10^{-6} Ω^{-1} cm^{-1} for a typical mixture of *N*-methyl pyrrolidone, acetone, and triethylamine). After being exposed to air for several hours (with $E = 0$), the conductance increased about fourfold, and, with $V \approx 100$ V, electrolysis occurred at the electrodes, producing visible bubbles. The conductance decreased to original value and the bubble formation ceased with prolonged passage of current through the sample (e.g., 10–30 min). Typically, for the polymer suspensions κ_{SP} was three- to fivefold larger than the value for dry solvent, and bubble formation could sometimes be observed.

The viscosity of the mixed solvents were determined at 25°C using a calibrated capillary viscometer, and the refractive index of the mixtures were measured at 25°C using an Abbe refractometer.

RESULTS

Data obtained on $R(q, c)$ obtained with a suspension of polymer I (see Table I) and dilutions thereof in composition 1, prepared by adding the solvent/nonsolvent mixture to the starting suspension, are shown in Figure 2. The correlation length $b(c)$ defined by eq. (13) was readily determined for each c. As shown in Figure 3, $b(c)$ was in the range 30–40 nm, and the

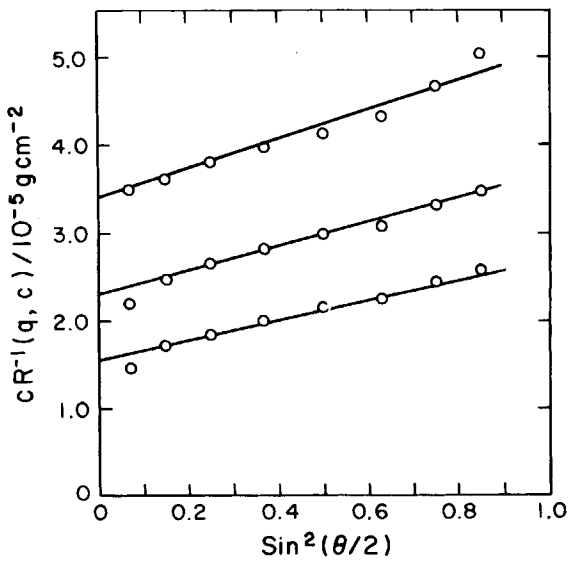

Fig. 2. The ratio $c/R(q, c)$ vs. $\sin^2\theta/2$ for emulsions of composition 1 (see Table I) for polymer concentrations of 0.28, 0.54, and 1.25 g/L from bottom to top.

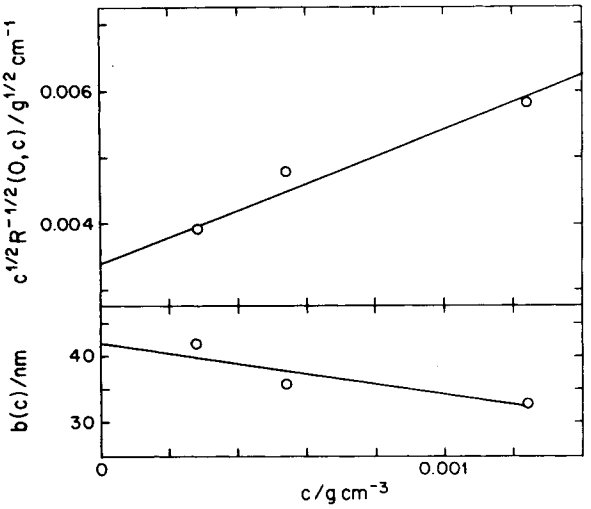

Fig. 3. Plots of $[c/R(0, c)]^{1/2}$ vs. c (upper) $b(c)$ vs. c (lower) for the data in Figure 2.

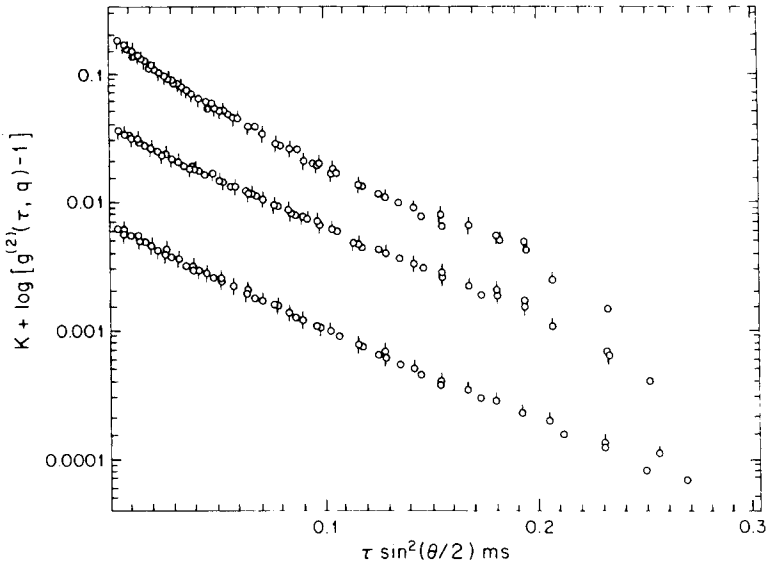

Fig. 4. The photon count autocorrelation function as $\log(g^{(2)}(\tau, q) - 1)$ vs. $\tau \sin^2\theta/2$ for emulsions of compositions 1 (see Table 1), with c (g/L) equal to 40, 4.0, and 1.0 from top to bottom, respectively. The constant K is 0, −0.87, and −1.69 from top to bottom. The pips identify scattering angles: (♀) 60°; (♁) 90°; (○) 120°.

limiting value $[c/R(0, c)]^{1/2}\{\partial[c/R(0, c)]/\partial c\}^{1/2}$ at infinite dilution was large, about 600 mL/g.

Examples of typical results for $g^{(2)}(\tau, q)$ obtained in self-beating experiments are shown in Figure 4. The data could be represented by the use of eq. (15) with one or two terms for all suspensions studied. The method used to determine the r_α and γ_α from data on $g^{(2)}(\tau, q)$ is discussed in detail elsewhere.[13] As shown by the superposition of data on $g^{(2)}(\tau, q)$ vs. τq^2 for a

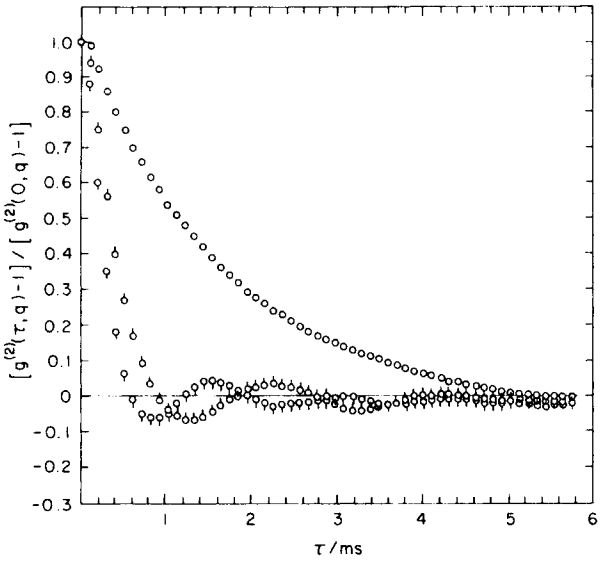

Fig. 5. The function $[g^{(2)}(\tau, q) - 1]/[g^{(2)}(0, q) - 1]$ vs. τ for an emulsion with composition 5 (see Table 1) and polymer concentration 8.0 g/L. The symbols designate applied potential E equal to zero (○) 69.7 V/cm; (◇), and 98.1 V/cm (▽).

range of θ (see Fig. 4), both a_α and r_α are independent of θ; the former behavior is frequently observed, but the latter is unexpected[5,13] (see below). The scattering properties of suspensions changed with time after preparation. For the systems studied, the scattering essentially stabilized after a period of no more than a few hours, such that further change in the scattering was small over a period of several days. Typically, for the freshly prepared emulsion the a_α tended to be larger than values found subsequently.

Examples of typical results obtained in reference beam experiments are shown in Figures 5 and 6, both for $E = 0$ and for $E > 0$. Values of a_α and r_α obtained in the former case agree with those found in self-beating experiments, as expected. With $E > 0$, the correlation function became a damped cosine function of the correlation time τ. In no case was more than one frequency component apparent in $g^{(2)}(\tau, q)$.

With prolonged imposition of the electric field, a layer of the suspended phase appears at one electrode (usually the anode). With such depleted solutions usually only one component was observed. An example of $g^{(2)}(\tau, q)$ for an emulsion prior to electrodeposition and after removal of about 80% of the polymer electrodeposition is shown in Figure 6, with entries for r_α and a_α in Table II.

As seen in Figures 5 and 6, the function $g^{(2)}(\tau, q)$ exhibits several maxima, occurring for τ equal to $m\tau_1$, with m an integer and τ_1 the time corresponding to the first maximum for $\tau > 0$. The function $g^{(2)}(\tau, q)$ is seen to be much smaller with $E > 0$ than for $E = 0$. The ratio τ_1/E was found to be independent of E.

The sample cell was translated vertically with respect to the scattering plane to determine whether $g^{(2)}(\tau, q)$ exhibited any variation, as might occur with an appreciable electroosmosis effect.[11] Except near the top of the cell,

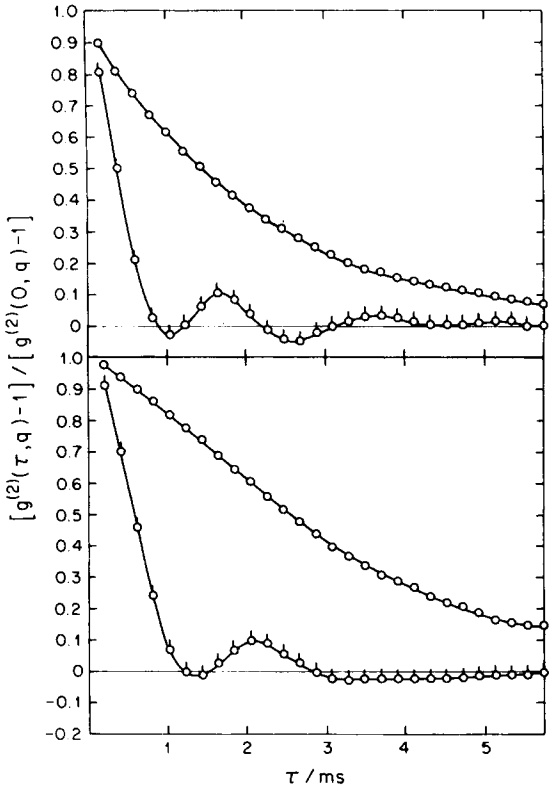

Fig. 6. The function $[g^{(2)}(\tau, q) - 1]/[g^{(2)}(0, q) - 1]$ vs. τ emulsions with composition 1: (upper) emulsion with concentration 6.2 g/L, and applied field E equal to zero (○) or 135.3 V/cm (◔); (lower) emulsion after depletion by electrodeposition ($c \approx 0.6$ g/L), with E equal to zero (○) or 176.5 V/cm (◔).

TABLE II
Parameters from Electrophoretic Light Scattering Studies[a]

Emulsion	c (g/L)	a_2 (nm)	r_2	a_1 (nm)	r_1	$\frac{[g^{(2)}(\tau_1) - 1]_E}{[g^{(2)}(\tau_1]_{E=0}}$[b]	$\hat{Z}_n$[c]	$\hat{Z}_w/\hat{Z}_n$[d]
1	6.20	12	0.26	68	0.74	0.32	20	1.06
1[e]	[e]	—	—	120	1.00	0.16	23	1.09
2	8.50	0.9	0.20	13	0.80	[f]	4.7	—
3	6.00	0.9	0.18	12	0.82	[f]	0.6	—
4	8.12	10	0.40	100	0.60	0.40	50	1.05
5	8.00	6.4	0.38	63	0.62	0.11	50	1.11
6	5.75	8.7	0.15	150	0.85	0.31	85	1.06

[a] Scattering angle of 20°.
[b] $\tau_1 = 2\pi/\Omega\hat{Z}_n$.
[c] Calculated with eq. (26).
[d] Calculated with eq. (28) with $\tau = \tau_1$.
[e] Suspension remaining following removal of most of the polymer from emulsion 1 by electrodeposition; c less than 1 g/L.
[f] Less than 0.05.

any such effect appeared to be small. In general, data were obtained using the middle or lower middle part of the cell.

Data obtained with several samples are summarized in Table II; the electrophoretic data are expressed in a notation discussed in the next section.

DISCUSSION

The suspensions prepared here comprise droplets of concentrated polymer solution dispersed in a mixed solvent, with the polymer concentration ρ in the droplet about 200 g/kg. The volume fraction ϕ of the droplets in the suspension is c/ρ, or about 0.03 for most of the suspensions used in electrophoretic scattering. The scattering from the dispersion is much larger than that for the solution prior to phase separation. Consequently, as discussed in the Introduction, it is concluded that the scattering arises from the droplets acting as the scattering particles, with M_w for the droplets much larger than M_w for the polymer chains.

In the following, we consider first the electrophoretic scattering to estimate the effective charge number $\hat{Z}$ per droplet—the relation between $\hat{Z}$ and the actual charge number Z is discussed below. Aspects of the static light scattering are then discussed in terms of the electrostatic interactions among the droplets, followed by discussion of the dependence of the dynamic scattering on scattering angle. As the electrophoretic data are qualitatively similar for all of the emulsions, the discussion will focus on emulsions of polymer 1 in the following since the data set on this composition is more complete, and it proved to be the most stable suspension.

Electrophoretic Scattering. Although $g^{(2)}(\tau, q)$ is not accurately an exponential function of τ over the entire span of τ studied, over the range of τ used to study the electrophoretic scattering $g^{(2)}(\tau, q)$ is essentially exponential, so that eq. (20) may be expressed in the form

$$g^{(2)}(\tau, q) - 1 \approx A \exp(-\gamma\tau) \int_0^\infty p(\hat{Z}) \cos(\Omega \hat{Z} \tau)\, d\hat{Z} \tag{24}$$

where $\Omega = eE \sin\theta / 3\eta_S \lambda_a$ with e the electron charge, A is constant, and γ and a are related through eq. (16). If the distribution of $\hat{Z}$ about its mean is symmetric, then eq. (24) may be put in the form

$$g^{(2)}(\tau, q) - 1 \approx A \exp(-\gamma\tau) \cos(\Omega \hat{Z}_n \tau) H(\Omega \hat{Z}_n \tau) \tag{25a}$$

$$H(\Omega \hat{Z}_n \tau) = \int_0^\infty p(\hat{Z}) \cos[\Omega\tau(\hat{Z} - \hat{Z}_n)]\, d\hat{Z} \tag{25b}$$

$$\hat{Z}_n = \int_0^\infty \hat{Z} p(\hat{Z})\, d\hat{Z} \tag{25c}$$

Thus, in this case the smallest value τ_0 of τ for which $g^{(2)}(\tau, q) - 1$ is zero is given by $\Omega \hat{Z}_n \tau_0 = \pi/2$, and τ_1, the smallest $\tau > 0$ for a maximum in $g^{(2)}(\tau, q)$, is given by $\Omega \hat{Z}_n \tau_1 \approx 2\pi$, providing means to compute $\hat{Z}_n$ as

$$\hat{Z}_n = \left[\frac{\lambda k T}{4eE \sin\theta}\right]\left[\frac{q^2}{\gamma\tau_0}\right] \approx \left[\frac{\lambda k T}{eE \sin\theta}\right]\left[\frac{q^2}{\gamma\tau_1}\right] \tag{26}$$

Values of $\hat{Z}_n$ calculated in this way were in the range 0.5–85, see Table II. Values of a computed from γ with eq. (16) are also entered in Table II (these a are referred to as a_1 in Table II.)

According to eq. (25), for $\tau = \tau_1 = 2\pi/\Omega\hat{Z}_n$,

$$g^{(2)}(\tau_1, q) - 1 = A \exp(-\gamma\tau_1) H(\Omega\hat{Z}_n\tau_1) \tag{27}$$

Since $H(\Omega\hat{Z}_n\tau)$ is unity for a system monodisperse in $\hat{Z}$, $g^{(2)}(\tau_1, q)$ should be independent of E for a monodisperse system. As seen in Figures 5 and 6, there is no $\tau > 0$ for which this condition is found for the system studied here, suggesting that the particles exhibit a distribution of $\hat{Z}$. Values of $\hat{Z}_n$ and $[g^{(2)}(\tau_1, q) - 1]_E/[g^{(2)}(\tau_1, q) - 1]_{E=0}$ are given in Table II for several samples.

If a Gaussian distribution is assumed for $\hat{Z}$ about its mean, then with eq. (25),

$$H(\Omega\hat{Z}_n\tau) = \exp\left[-\frac{(\Omega\hat{Z}_n\tau)^2}{2}\left(\frac{\hat{Z}_w}{\hat{Z}_n} - 1\right)\right] \tag{28}$$

where $\hat{Z}_w$ and $\hat{Z}_n$ are the weight and number averages of $\hat{Z}$ with respect to the distribution $p(\hat{Z})$ [e.g., see eq. (25c) for $\hat{Z}_n$]. Thus, even modest deviation of $\hat{Z}_w/\hat{Z}_n$ from unity can cause a large suppression in $g^{(2)}(\tau, q)$ for $\tau > 0$. For example, $g^{(2)}(\tau_1, q) - 1$ is reduced by one fourth if $\hat{Z}_w/\hat{Z}_n = 1.07$, or to one tenth the value in the absence of a field if $\hat{Z}_w/\hat{Z}_n = 1.12$. Values of $\hat{Z}_w/\hat{Z}_n$ are entered in Table II as calculated for an *assumed* Gaussian $p(\hat{Z})$. On the basis of this analysis, it is concluded that the droplets exhibit heterogeneity of charge number $\hat{Z}$, as might be expected, with the average number $\hat{Z}_n$ being only modest in magnitude.

Static Scattering. Based on the evidence that the droplets are charged, we first estimate the functions $W(q, 0)$ and Γ_2 in eqs. (9) and (10), respectively, with $V(r)$ for spheres with identical radius R and charge number Z[15]:

$$V(r)/kT = \begin{cases} \infty, & r < 2R \\ F\dfrac{\exp(-\kappa r)}{\kappa r}, & r \geq 2R \end{cases} \tag{29a}$$

$$F = F_0 \frac{\kappa R}{(1 + \kappa R)^2} \exp(2\kappa R) \tag{29b}$$

where $F_0 = Z^2 L_B/R$. Here the Debye screening length κ^{-1} depends on the number n_i of coions or counterions with charge Z_i:

$$\kappa^2 = 4\pi L_B \sum n_i Z_i^2 \tag{30}$$

The Bjerrum length L_B, equal to $e^2/\epsilon kT$ with ϵ the dielectric constant, is about 2.2 nm for the systems studied.

The specific conductance κ_{SP} provides a measure of the ionic radius κ^{-1} if it is assumed that conduction occurs as a result of monovalent counterions and

coions, so that

$$\kappa^{-1} \approx [\Lambda/4\pi N_A L_B \kappa_{SP}]^{1/2} \tag{31}$$

with Λ the molar conductance. Thus, for the "dry" solvent, $\kappa^{-1} \approx 15$ nm (ion concentration of 0.4 mmol/L), using the typical value[16] $\Lambda = 100$ Ω^{-1} cm^2 mol^{-1}; for a typical suspension, $\kappa^{-1} \approx 30$ nm on the same basis. Since the nature of the diffusing coions and counterions contributing to κ_{SP} is unknown (see below), it is possible that Λ could deviate from the "typical" value cited, but should be in the range 10–200 Ω^{-1} cm^2 mol^{-1} in any case[16] (see below).

The product κR appears in the relation between the true charge Z and the apparent charge $\hat{Z}$ determined in electrophoretic light scattering[11]:

$$\hat{Z} \approx Z\frac{\sigma(\kappa R)}{(1 + \kappa R)} \tag{32}$$

where σ is a function with values between 1 and 1.5.[11,17] With $a_1 \approx 70$ nm taken as R, and $\kappa^{-1} \approx 15$ nm, $\kappa R \approx 4.67$ and $Z \approx 5.67\hat{Z}$. It may be noted that a distribution of R will lead to a distribution of $\hat{Z}$ according to eq. (32) even if Z (or Z/R) is constant.

With the use of eq. (29), Γ_2 may be determined by numerical evaluation of eq. (10) for monodisperse, charged, impenetrable spheres to obtain a result of the form

$$\Gamma_2 = \Gamma_2^{(H)}[1 + \gamma_2(F_0, \kappa R)] \tag{33}$$

where $\Gamma_2^{(H)} = 16\pi R^3 N_A/3M$ is the result for zero charge. Alternatively, $\Gamma_2^{(H)} = 4/\rho$, or $\Gamma_2^{(H)} \approx 20$ mL/g for the dispersed droplets. The function $\gamma_2(F_0, \kappa R)$ is discussed in the Appendix. For large κR, γ_2 tends to zero, and for small κR, $(\kappa R)^3\gamma_2$ is a function of F alone:[18]

$$\lim_{\kappa R=0} (\kappa R)^3\gamma_2 = 3F/8\beta(F) \tag{34a}$$

$$\beta(F) \approx 1 + F^{5/8}/4(2)^{1/2} \tag{34b}$$

where eq. (34b) is an empirical representation of numerical values of $\beta(F)$. For intermediate κR, γ_2 cannot be expressed in terms of F alone. In general, over a limited variation of the parameters κ, R and Z, one can write

$$\delta \ln \gamma_2 = a\,\delta \ln R + b\,\delta \ln \kappa + c\,\delta \ln Z \tag{35}$$

For the nominal values $R = a = 70$ nm, $\kappa^{-1} = 15$ nm, and $\hat{Z} = 20$ reported for sample I, $\gamma_2 = 1.0$, $a = 1.8$, $b = 1.8$, and $c = 0.8$. If $(\partial[Kc/R(C,0]^{1/2}/\partial c)/[Kc/R(c,0]^{1/2})$ at infinite dilution is accepted as Γ_2, then $\Gamma_2 = 600$ mL/g, and $\gamma_2 \approx 29$. The discrepancy between the latter estimate of γ_2 and the calculated value (1.0), is too large to attribute to errors in R, κ, or $\hat{Z}$. Other contributing factors to the discrepancy including the effects

of heterogeneity of R and Z, and the variation of these parameters with c, are discussed in the following.

With heterogeneity in R or Z, the second virial coefficient becomes[5,7]

$$\Gamma_{2,LS} = \frac{2\pi N_A}{M_w} \sum_i \sum_j B_{ij} M_i M_j w_i w_j \tag{36}$$

$$B_{ij} = (M_i M_j)^{-1} \int_0^\infty r^2 \left[1 - \exp\left(-V_{ij}(r)/kT\right)\right] dr \tag{37}$$

For a monodisperse system, $V_{ij}(r)$ is given by eq. (29), and eq. (33) for Γ_2 is recovered. The potential for spheres heterodisperse in R and Z has been discussed,[19] but is too complex for out limited purpose. Rather, to investigate the effects of heterogeneity on $\Gamma_{2,LS}$, two simplifications are adopted: (1) the surface potential on all spheres is taken to be independent of R, so that Z/R is constant, and (2) the convenient approximation $B_{ij} = (B_{ii}B_{jj})^{1/2}$ is used. The latter leads to reasonable approximations to $\Gamma_{2,LS}^{(H)}$ for hard spheres, for example. Further, with the assumption of constant Z/R for all particles, inspection of eq. (33) showns that B_{ii} can be expressed in the form

$$B_{ii} = \frac{8}{3M_i^2} \cdot R_i^3 \left[1 + (R_0/R_i)^\nu\right]^2 \tag{38}$$

where the constants ν and R_0 depend on κ and the assumed Z/R. With these simplifications, evaluation of eq. (36) gives

$$\Gamma_{2,LS} \approx \frac{4}{\rho} \cdot \left[\frac{R_{(3/2)}}{R_{(3)}}\right]^3 \left[1 + \left[\frac{R_{(\epsilon)}}{R_{(3/2)}}\right]^{3/2} \left[\frac{R_{(4)}^4}{R_{(3)}^3 R_{(\epsilon)}}\right]^\nu \left[\frac{R_0}{a_{LS}}\right]^\nu\right]^2 \tag{39}$$

where $\epsilon = (3 - 2\nu)/2$, and use is made of the relation $M_w = 4\pi N_A R_{(3)}^3 \rho/3$ obtained on the assumption that the density ρ of the polymer in the droplets is independent of their size. Here, $R_{(a)}$ is calculated from

$$R_{(a)}^a = \sum R_i^a w_i \tag{40}$$

and a_{LS} is calculated with eqs. (6) and (8) with the assumption that $a_i = R_i$, to give

$$a_{LS} = R_{(4)}^4/R_{(3)}^3 \tag{41}$$

By comparison, with the assumption made, $\Gamma_{2,LS}^{(H)}$ is given by eq. (39) with R_0 equal to zero. If the distribution of R follows a log-normal function,[20] then $R_{(a)} \propto \exp[(a + 2)\beta^2/2]$, so that

$$\Gamma_{2,LS} \approx \frac{4}{\rho} \cdot \exp\left(-\frac{3}{4}\beta^2\right) \left\{1 + \exp\left[\left(-\frac{77}{72} + \frac{7}{2}\nu\right)\beta^2\right] \left(\frac{R_0}{a_{LS}}\right)^\nu\right\}^2 \tag{42}$$

With the log-normal distribution, $R_w/R_n = R_{(1)}/R_{(-1)} = \exp\beta^2$. For $Z/R =$

$114/70 = 1.63\ \text{nm}^{-1}$, eq. (38) applies with $\nu \approx 7/6$ and $R_0 = 31$ nm. Use of eq. (42) and these parameters gives $R_w/R_n = 2.36$ to force agreement between calculated and observed values of $\Gamma_{2,LS}$.

As seen below, the dispersion of R discussed above appears to be reasonable in terms of the observed dependence of $b(c)$ on c. However, for completeness, we estimate the magnitude of the variation of molecular weight M_w or average radius $R_{(3)}$ that could correspond to the observed dependence of $R(c,0)$ on c by use of the expression

$$\frac{\partial \ln c/R(c,0)}{\partial \ln c} \approx -3\frac{\partial \ln R_{(3)}}{\partial \ln c} + \frac{2\Gamma_{2,LS}c}{1+2\Gamma_{2,LS}c} \times\left\{1 + \frac{\partial \ln \Gamma_{2,LS}}{\partial \ln R_{(3)}}\frac{\partial \ln R_{(3)}}{\partial \ln c}\right\} \tag{43}$$

For the range of c studied with emulsion 1, $\partial \ln c/R(c,0) \approx 0.5$ and $2\Gamma_{2,LS}c/(1+2\Gamma_{2,LS}c) \approx 0.15$ based on the computed $\Gamma_{2,LS}$. For $\kappa R \approx 3$, $\partial \ln \Gamma_{2,LS}/\partial \ln_{2,LS}/\partial \ln R \approx -0.52$, making use of eq. (38). Combination of these parameters gives $\partial \ln(R^3)w/\partial \ln c \approx -0.27$, or a 10% decrease in the average dimension over the range of c studied.

The function $W(q,0)$ appearing in the correlating length $b(c)$ for low c may be evaluated for a monodisperse system using $V(r)$ given by eq. (29), with the result

$$W(q,0) = 1 - \tfrac{2}{5}R^2q^2[1 - \omega(F_0, \kappa R)] + \cdots \tag{44}$$

For large κR, $\omega \ll 1$, giving the well-known result for impenetrable spheres [see eq. (12)]. For small κR, $\omega \gg 1$ and $(\kappa R)^2\,\omega$ is a function of F alone:

$$\lim_{\kappa R=0} \omega = \frac{5}{12(\kappa R)^2} \cdot \psi(F) \tag{45a}$$

$$\psi(F) \approx 16.56\beta^{1/2}(F) \tag{45b}$$

where $\beta(F)$ is given by eq. (34b) (see Appendix). With use of eqs. (6), (14), and (44), the correlation length $b(c)$ for low c is given by

$$b^2(c) \approx \frac{3}{5}R^2\frac{1}{1+(3+2\omega)\Gamma_2 c} \tag{46}$$

Since $\omega > 0$, according to eq. (46), $b(c)$ is expected to decrease with increasing c, in contrast with the experimental result for emulsion 1, for which $b(c)$ is about constant over the range of c studied. For example, with $R = 70$ nm, $\kappa^{-1} = 15$ nm, and $Z = 20$, $\omega = 2.6$. The effects of heterogeneity of R and Z may account for the discrepancy. A full treatment of this is beyond our scope, but a simplified model can reveal the qualitative nature of the effect. Thus, for small q and c,

$$b^2(c) \approx \frac{3}{5}a_{LS}^2 b_1\{1 + [(3+2\bar{\omega})b_2 - 1](2\Gamma_{2,LS}c) + \cdots\}^{-1} \tag{47}$$

where $\bar{\omega}$ is an average of ω. For uncharged impenetrable spheres ($\bar{\omega} = 0$ and $\Gamma_{2,LS} = \Gamma_{2,LS}^{(H)}$),

$$b_1 = R_{(5)}^5 R_{(3)}^3 / R_{(4)}^8 \tag{48}$$

$$b_2 = \frac{1 + 5\left[R_{(4)}^4 R_{(1)}/R_{(5)}^5\right] + 10\left[R_{(3)}^3 R_{(2)}^2/R_{(5)}^5\right]}{4\left[1 + 3R_{(2)}^2 R_{(1)}/R_{(3)}^3\right]} \tag{49}$$

For the log-normal distribution of R used above in the discussion of $\Gamma_{2,LS}$, $b_2 \approx 0.20$, and the dependence of $b(c)$ on c should be suppressed. The situation is apparently similar for the charged droplets since $b(c)$ is essentially independent of c. For this same distribution, $b_1 = \exp\beta^2$, or 2.36 for the β used above. Consequently, $b(c)$ is expected to be nearly equal to a_{LS}, as observed for this system.

Dependence of the Dynamic Scattering on Angle. Finally, an unusual feature of the data on $g^{(2)}(\tau, q)$ obtained with $E = 0$ may be noted in Figure 4, namely, for $c = 6.2$ g/L, the data could be fitted by eq. (15) with $\alpha = 1, 2$, but r_1 and $r_2 = 1 - r_1$, did not depend on q as is usually expected if the sizes are large enough that $P(q) < 1$. Thus, if the r_α are attributed to "components," then with the use of Eqs. (3), (7), and (18),

$$r_\alpha \approx K_r \left(\frac{cM}{1 + 2\Gamma_{2,LS}c} \left\{ 1 + \frac{1}{5} b_1 q^2 R^2 \left[1 + 2\Gamma_{2,LS}c(1 - (3 - 2\bar{\omega})b_2) \right] \right\}^{-1} \right)_\alpha \tag{50}$$

where K_r is a normalization constant and

$$(\Gamma_{2,LS})_\alpha c_\alpha \approx 4\phi_\alpha (1 + \bar{\gamma}_{2,\alpha}) \tag{51}$$

In these expressions, $\bar{\omega}_\alpha$ and $\bar{\gamma}_{2,\alpha}$ represent interaction parameters suitably averaged over the species present. Thus, for example, with two "components," r_1/r_2 is expected to vary with q according to eq. (50) unless $qR \ll 1$. An explanation for the unusual independence of the observed r_1/r_2 on q may be related to the dispersion in $\hat{Z}$ encountered above. In a theoretical study[21] of $g^{(2)}(\tau, q)$ for droplets monodisperse in radius R, but with $n/2$ spheres per unit volume, each bearing charge number $Z + \delta$, and another $n/2$ spheres each bearing charge $Z - \delta$, it was found that $[g^{(2)}(\tau, q) - 1]^{1/2}$ comprised two exponential terms, with

$$\frac{r_1}{r_2} = \left[\frac{\delta}{Z}\right]^2 \frac{1 + 2nIZ^2}{1 + nI(Z^2 - \delta^2)} \approx \left[\frac{\delta}{Z}\right]^2 \frac{\gamma_2}{\gamma_1} \tag{52}$$

$$\gamma_2 = \gamma_1 \left[1 + nI(Z^2 + \delta^2)\right] \tag{53}$$

$$\gamma_1 = q^2 kT / 6\pi\eta_S R \tag{54}$$

Here, I is a measure of the strength of the electrostatic interaction.[21] With eq. (52), r_1/r_2 is independent of q, and, as n is made small, r_2 tends to unity.

Furthermore, as n tends to zero, γ_2 tends to γ_1. This behavior is qualitatively similar to the variation of $g^{(2)}(\tau, q)$ with q and c found for emulsion 1, suggesting that the origin of the observed behavior may involve effects of charge distribution among the droplets. The electrophoretic light scattering data discussed above are consistent with this postulate of a distribution of charge among the droplets. On dilution, $g^{(2)}(\tau) - 1$ becomes nearly exponential, as would be expected with eqs. (52)–(54) with decreasing n.

Remarks on Emulsion Electrodeposition. The formation of a useful coating through electrodeposition of polymer from an emulsion depends on several factors including: the electric charge on the suspended droplets; the stability of the emulsion; the electrical current during the electrodeposition; the stability of the layer formed during electrodeposition; and the integrity of the final dry coating. Several of these factors may be addressed for the emulsions studied here.

The use of reagents with low conductivity provides for low electrical current (i.e., low power consumption). Comparison of κ_{SP} for the solvents and the emulsion shows that most, if not nearly all, of the power consumption is extraneous to the formation of a polymer layer during electrodeposition. Indeed, a layer could be formed below a porous frit isolated from the electrode, showing that polymer reactions at the electrode are not essential. This feature is probably important in the formation of a relatively thick layer. The charge on the droplets may inhibit their coalescence in the layer. Thus, the material in a layer will slowly disperse on suppression of the applied field. The power consumption in forming the layer (less the extraneous power consumed in small ion transport) may be best considered as that required to charge a capacitor comprising the charged droplets and their counterions in an electrically neutral milieu. In this model the useful current decreases to zero as formation of the layer is completed by depletion of the polymer available in the emulsion. The power consumption P per unit electrode area at time t may be expressed as

$$P = \frac{\partial W}{\partial t} = \frac{\partial l}{\partial t}\frac{\partial W}{\partial l} \tag{55}$$

where W is the work (per unit area) required to bring a droplet to the surface layer and l is the thickness of the layer. As a first approximation, the principal contribution to $\partial W/\partial l$ is taken to arise from the difference in free energy of droplets closely spaced in the layer as compared with droplets in the dispersion. Thus,

$$\partial W/\partial l \approx [V(l_L) - B(l_D)]/2R^3$$

where l_L and l_D are the average center-to-center distances of the droplets in the layer and in the dispersed phase, respectively, and $V(r)$ is given by eq. (29). The distance l_L should be about equal to $2R + \kappa^{-1} \approx 2R$, and $l_D = R(4\pi/3\phi)^{1/3}$. With eq. (55), $\partial W/\partial l$ should increase as the solution is depleted and $V(l_D)$ approaches zero, and in consequence the deposition rate $\partial l/\partial t$ should decrease. Further, the parameters influencing $\partial W/\partial l$ are those affecting $V(r)$; e.g., κ, L_B, $\hat{Z}$, and κR. Thus, for large l_D, $\partial W/\partial l \approx (L_B\hat{Z}^2/2R^4)kT$.

The origin of the charge on the droplets is obscure. Possibilities include the adsorption of adventitious ions introduced via impurities on glassware, in solvents, etc., the adsorption of ions created by reaction of the solvents or the polymer with water, carbon dioxide, or oxygen adsorbed from the atmosphere, or tribologic effects among the droplets during mixing.[22] The observation that κ_{SP} is similar for the solvents and the solutions implicates either adventitious ions or reaction products from the solvents. The low level of ions involved (ca. 1 mmol/L based on κ_{SP}) is consistent with such a source. It appears, however, that different compositions result in different Z, despite more or less similar methods of dispersion preparation, suggesting tribologic effects may also be important.

A liquid nature for the droplets may be important to the integrity of the final coating. With time, the droplets may coalesce through discharge of their charge, leading to a liquid layer rich in polymer. The coating may then be formed by exposure to nonsolvent, causing the polymer to precipitate as a dense layer.

APPENDIX

The functions γ_2 and ω involve integrals of the type

$$I_n(F_0, z) = \frac{n}{(2z)^n} \int_{2z}^{\infty} dx\, x^{n-1} \{1 - \exp[-F\exp(-x)/x]\} \tag{56}$$

$$F = F_0 \frac{z \exp 2z}{(1+z)^2} \tag{57}$$

Thus, with the use of eqs. (9), (10), (11), and (29),

$$\gamma_2 = I_3(F_0, \kappa R) \tag{58}$$

$$\omega = \frac{I_5(F_0, \kappa R) + I_3(F_0, \kappa R)}{1 + I_3(F_0, \kappa R)} \tag{59}$$

As z tends to zero, $z^n I_n(F_0, z)$ tends to a limiting value that depends only on F:

$$\lim_{z=0} z^3 I_3(F_0, z) = \frac{3}{8} \frac{F}{\beta(F)} \tag{60}$$

$$\lim_{z=0} z^5 I_5(F_0, z) = \frac{5}{32} \cdot \frac{F}{\beta(F)} \psi(F) \tag{61}$$

$$\lim_{z=0} \frac{z^5 I_5(F_0, z)}{z^3 I_3(F_0, z)} = \frac{5}{12} \psi(F) \tag{62}$$

Use of eqs. (58) and (59) give eqs. (34a) and (45a) of the text, respectively. Inspection of numerical values of $\psi(F)$ and $\beta(F)$ provide the estimates given as eqs. (34b) and (45b) of the text, respectively. With increasing κR, neither $I_3(F_0, \kappa R)$ or $I_5(F_0, \kappa R)$ can be expressed as functions of F alone, making γ_2 and ω functions of both F_0 and κR. Plots of $(2\kappa R)^3 I_3(F_0, \kappa R)/3F_0$ and $(2\kappa R)^3 I_5(F_0, \kappa R)/5F_0$ vs. κR are shown in Figure 7.

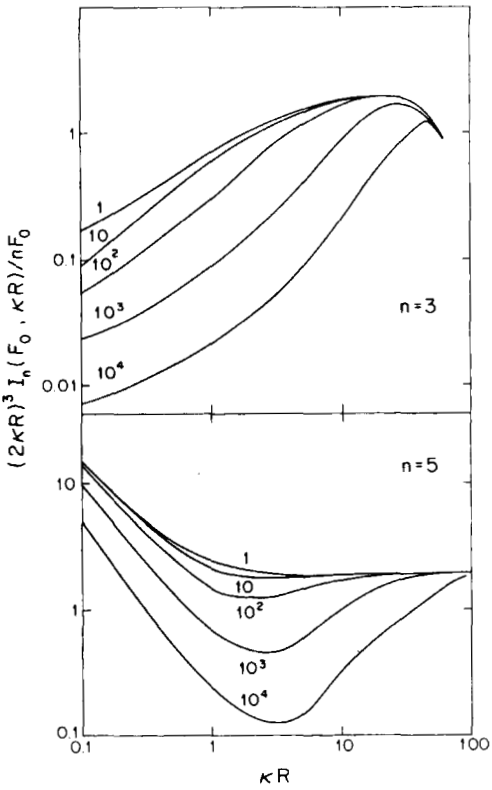

Fig. 7. The functions $(2\kappa R)^3 I_n(F_0 \kappa R)/nF_0$ vs. κR for the indicated values of F_0: (upper) $n = 3$; (lower) $n = 5$.

Partial support for this study was provided by a grant from the Westinghouse Research and Development Center, Pittsburgh, PA. Some of the work reported represents a part of the M.S. thesis submitted to the Department of Chemistry by R. L. F. in partial completion of degree requirements.

References

1. P. J. Flory, *Principles of Polymer Chemistry*, Cornell University Press, Ithaca, NY, 1953.
2. W. M. Alvino and L. C. Scala, *J. Appl. Polym. Sci.*, **27**, 341 (1982).
3. W. M. Alvino, T. J. Fuller, and L. C. Scala, *J. Appl. Polym. Sci.*, **28**, 267 (1983).
4. R. J. Berne and R. Pecora, *Dynamic Light Scattering*, Wiley-Interscience, New York, 1976.
5. G. C. Berry, in *Encylopedia of Polymer Science and Engineering*, Wiley, New York, 1987, Vol. 9.
6. J. M. Schurr, *CRC Crit. Rev. Biochem.*, **4**, 371 (1977).
7. E. F. Casassa and G. C. Berry, in *Polymer Molecular Weights*, Part 1, P. E. Slade, Jr., Ed., Dekker, New York, 1975, Chap. 5.
8. W. Burchard, *Adv. Polym. Sci.*, **48**, 1 (1983).
9. B. H. Zimm, *J. Chem. Phys.*, **16**, 1093, 1099 (1948).
10. A. Guinier and G. Fournet, *Small-Angle Scattering of X-Rays*, Transl. by C. B. Walker, Wiley, New York, 1965; University Microfilms, Ann Arbor, MI.
11. B. R. Ware, *Adv. Coll. Interface Sci.*, **4**, 1 (1974).
12. C. C. Lee, S.-G. Chu, and G. C. Berry, *J. Polym. Sci., Polym. Phys. Ed.*, **21**, 1573 (1983).
13. Y. Einaga and G. C. Berry, in *Microdomains in Polymer Solutions*, P. Dubin, Ed., Plenum, New York, 1985, Chap. 11.

14. S. Qutubuddin, C. A. Miller, G. C. Berry, T. Fort, Jr., and A. Hussam, in *Surfactants in Solution*, K. Mittal and B. Lindman, Eds., Plenum, 1984, Vol. 3, p. 1693.

15. D. G. Neal, D. Purich, and D. S. Cannell, *J. Chem. Phys.*, **80**, 3469 (1984).

16. A. K. Covington and T. Dickinson, *Physical Chemistry of Organic Solvent Systems*, Plenum, 1973

17. D. C. Henry, *Proc. Roy. Soc. (London)*, **A133**, 106 (1931).

18. D. Stigter and T. L. Hill, *J. Phys. Chem.*, **63**, 551 (1959).

19. G. M. Bell, S. Levine, and L. N. McCarney, *J. Coll. Interface Sci.*, **33**, 335 (1970).

20. G. C. Berry, in *Encyclopedia of Materials Science and Engineering*, M. B. Bever, Ed., Pergamon, Oxford, 1986, p. 3759.

21. G. D. J. Phillies, *Macromol.*, **9**, 447 (1976)

22. J. Lykelma, in *Colloidal Dispersions*, J. W. Goodwin, Ed., Roy. Soc. Chem., Special Publ. No. 43, Dorset Press, Dorchester, U.K., 1982, p. 50.

Received May 14, 1987
Accepted June 17, 1987